INTERFACE

rsif.royalsocietypublishing.org

On the biomechanical analysis of the calories expended in a straight boxing jab

T. I. Zohdi

Department of Mechanical Engineering, University of California, Berkeley, CA 94720-1740, USA

TIZ, 0000-0002-0844-3573

Research

Check for updates

Cite this article: Zohdi TI. 2017 On the biomechanical analysis of the calories expended in a straight boxing jab. *J. R. Soc. Interface* **14**: 20170153.
http://dx.doi.org/10.1098/rsif.2017.0153

Received: 1 March 2017
Accepted: 20 March 2017

Subject Category:
Life Sciences–Engineering interface

Subject Areas:
bioengineering

Keywords:
boxing, kinematics, energy

Author for correspondence:
T. I. Zohdi
e-mail: zohdi@berkeley.edu

Boxing and related sports activities have become a standard workout regime at many fitness studios worldwide. Oftentimes, people are interested in the calories expended during these workouts. This note focuses on determining the calories in a boxer's jab, using kinematic vector-loop relations and basic work–energy principles. Numerical simulations are undertaken to illustrate the basic model. Multi-limb extensions of the model are also discussed.

1. Introduction: kinematic vector loop representation of a jab

Fitness enthusiasts are keenly interested in the calories expended during non-standard work regimes involving martial arts, boxing and related sports [1–6]. As an example of how to determine the calories expended in a simple straight boxer's jab (figure 1) from basic principles, we employ a combined kinematic and energy analysis, by drawing on methods used in the robotics literature [7–16].

Accordingly, consider the idealization of a jab illustrated in figures 1–3 as a linkage. Viewing the boxer from the top, we can analyse the motion of the components of a linkage by applying a closed vector loop that traverses the upper arm, forearm and fist, generating a slider crank mechanism capable of describing a straight left jab. It is made up of a block mass (fist) with mass m attached by two rigid rods (upper arm and forearm). The angle $\theta_4 = \theta_c$ is controlled. The position vector loop around the linkage is given by

$$\boldsymbol{r}_1 + \boldsymbol{r}_2 + \boldsymbol{r}_3 + \boldsymbol{r}_4 = \boldsymbol{0}. \tag{1.1}$$

Differentiating, a velocity vector loop is generated

$$\dot{\boldsymbol{r}}_1 + \dot{\boldsymbol{r}}_2 + \dot{\boldsymbol{r}}_3 + \dot{\boldsymbol{r}}_4 = \boldsymbol{0}. \tag{1.2}$$

In component form, for a planar mechanism, we have, for the x-components of position

$$r_1 \cos\theta_1 + r_2 \cos\theta_2 + r_3 \cos\theta_3 + r_4 \cos\theta_4 = 0 \tag{1.3}$$

and for the y-components of position

$$r_1 \sin\theta_1 + r_2 \sin\theta_2 + r_3 \sin\theta_3 + r_4 \sin\theta_4 = 0, \tag{1.4}$$

where $r_i = \|\boldsymbol{r}_i\| = \sqrt{\boldsymbol{r}_i \cdot \boldsymbol{r}_i}$ (for $i = 1, 2, 3, 4$) and all angles are measured anti-clockwise from horizontal right (figure 1). The two unknowns are r_2 and θ_3. The velocity unknowns are $\dot{r}_2$ and $\dot{\theta}_3$, and can be subsequently found from differentiating the component equations of equation (1.1), yielding, for the x-components of velocity:

$$\begin{aligned} &\dot{r}_1 \cos\theta_1 - r_1\dot{\theta}_1 \sin\theta_1 + \dot{r}_2 \cos\theta_2 - r_2\dot{\theta}_2 \sin\theta_2 \\ &\quad + \dot{r}_3 \cos\theta_3 - r_3\dot{\theta}_3 \sin\theta_3 + \dot{r}_4 \cos\theta_4 - r_4\dot{\theta}_4 \sin\theta_4 = 0 \end{aligned} \tag{1.5}$$

and for the y-components of velocity:

$$\begin{aligned} &\dot{r}_1 \sin\theta_1 + r_1\dot{\theta}_1 \cos\theta_1 + \dot{r}_2 \sin\theta_2 + r_2\dot{\theta}_2 \cos\theta_2 \\ &\quad + \dot{r}_3 \sin\theta_3 + r_3\dot{\theta}_3 \cos\theta_3 + \dot{r}_4 \sin\theta_4 + r_4\dot{\theta}_4 \cos\theta_4 = 0. \end{aligned} \tag{1.6}$$

THE ROYAL SOCIETY PUBLISHING

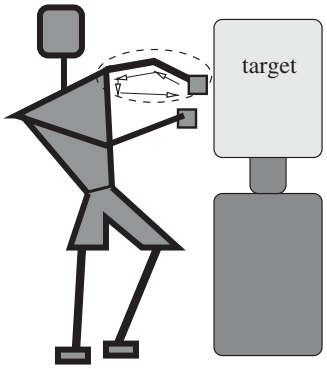

Figure 1. The motivation for the system to be modelled.

2. Solution algorithm

A solution can be determined in closed form by writing

$$\boldsymbol{r}_3 = -\boldsymbol{r}_1 - \boldsymbol{r}_2 - \boldsymbol{r}_4 \tag{2.1}$$

and taking the inner product $\boldsymbol{r}_3 \cdot \boldsymbol{r}_3$,

$$\boldsymbol{r}_3 \cdot \boldsymbol{r}_3 = \|\boldsymbol{r}_3\|^2 = (\boldsymbol{r}_1 + \boldsymbol{r}_2 + \boldsymbol{r}_4) \cdot (\boldsymbol{r}_1 + \boldsymbol{r}_2 + \boldsymbol{r}_4), \tag{2.2}$$

which yields

$$\boldsymbol{r}_3 \cdot \boldsymbol{r}_3 = \|\boldsymbol{r}_1\|^2 + \|\boldsymbol{r}_2\|^2 + \|\boldsymbol{r}_4\|^2 + 2\boldsymbol{r}_1 \cdot \boldsymbol{r}_4 + 2\boldsymbol{r}_2 \cdot \boldsymbol{r}_4 + 2\boldsymbol{r}_1 \cdot \boldsymbol{r}_2. \tag{2.3}$$

Since $\boldsymbol{r}_1 \cdot \boldsymbol{r}_2 = 0$ and using standard trigonometric identities we obtain

$$\begin{aligned}\|\boldsymbol{r}_3\|^2 = {} & \|\boldsymbol{r}_1\|^2 + \|\boldsymbol{r}_2\|^2 + \|\boldsymbol{r}_4\|^2 + 2\|\boldsymbol{r}_1\|\|\boldsymbol{r}_4\| \cos(\theta_1 - \theta_4) \\ & + 2\|\boldsymbol{r}_2\| \, \|\boldsymbol{r}_4\| \cos(\theta_2 - \theta_4),\end{aligned} \tag{2.4}$$

where $\theta_2 = 0$ and $\theta_1 = 3\pi/2$. Rearranging terms yields a quadratic equation

$$a\|\boldsymbol{r}_2\|^2 + b\|\boldsymbol{r}_2\| + c = 0, \tag{2.5}$$

where $a = 1$ and

$$b = 2\|\boldsymbol{r}_4\| \cos(-\theta_4) \tag{2.6}$$

and

$$c = \|\boldsymbol{r}_1\|^2 + \|\boldsymbol{r}_4\|^2 + 2\|\boldsymbol{r}_1\| \, \|\boldsymbol{r}_4\| \cos\left(\frac{3\pi}{2} - \theta_4\right) - \|\boldsymbol{r}_3\|^2. \tag{2.7}$$

The quadratic equation can be solved for the length of $\boldsymbol{r}_2$

$$\|\boldsymbol{r}_2\| = \frac{-b \pm \sqrt{b^2 - 4ac}}{2a}. \tag{2.8}$$

This then leads to the solution of the angle θ_3

$$\begin{aligned}\theta_3 &= \cos^{-1} \frac{(-\|\boldsymbol{r}_1\| \cos\theta_1 - \|\boldsymbol{r}_2\| \cos\theta_2 - \|\boldsymbol{r}_4\| \cos\theta_4)}{\|\boldsymbol{r}_3\|} \\ &= \cos^{-1} \frac{(-\|\boldsymbol{r}_2\| - \|\boldsymbol{r}_4\| \cos\theta_4)}{\|\boldsymbol{r}_3\|},\end{aligned} \tag{2.9}$$

where, as stated before, θ_4 is controlled. The larger of the two roots in both equations is the correct one. Since $\dot{r}_1 = 0$, $\dot{r}_3 = 0$, $\dot{r}_4 = 0$, $\dot{\theta}_1 = 0$, $\dot{\theta}_2 = 0$, $\dot{\theta}_4 =$ controlled, we have

$$\dot{r}_2 \cos\theta_2 - r_3\dot{\theta}_3 \sin\theta_3 = r_4\dot{\theta}_4 \sin\theta_4 \tag{2.10}$$

and

$$\dot{r}_2 \sin\theta_2 + r_3\dot{\theta}_3 \cos\theta_3 = -r_4\dot{\theta}_4 \cos\theta_4. \tag{2.11}$$

In matrix form

$$\begin{bmatrix} \cos\theta_2 & -r_3 \sin\theta_3 \\ \sin\theta_2 & r_3 \cos\theta_3 \end{bmatrix} \begin{Bmatrix} \dot{r}_2 \\ \dot{\theta}_3 \end{Bmatrix} = \begin{Bmatrix} r_4\dot{\theta}_4 \sin\theta_4 \\ -r_4\dot{\theta}_4 \cos\theta_4 \end{Bmatrix}, \tag{2.12}$$

which yields

$$\begin{Bmatrix} \dot{r}_2 \\ \dot{\theta}_3 \end{Bmatrix} = \begin{bmatrix} \cos\theta_2 & -r_3 \sin\theta_3 \\ \sin\theta_2 & r_3 \cos\theta_3 \end{bmatrix}^{-1} \begin{Bmatrix} r_4\dot{\theta}_4 \sin\theta_4 \\ -r_4\dot{\theta}_4 \cos\theta_4 \end{Bmatrix}. \tag{2.13}$$

3. Energy principles

One can immediately post-process the kinetic energy in the system as

$$T(t) = \sum_{i=1}^{\text{masses}} \frac{1}{2} m_i \boldsymbol{v}_i(t) \cdot \boldsymbol{v}_i(t) + \sum_{i=1}^{\text{links}} \frac{1}{2} I_i \dot{\theta}_i^2(t), \tag{3.1}$$

where in this specific case

$$\sum_{i=1}^{\text{masses}} \frac{1}{2} m_i \boldsymbol{v}_i(t) \cdot \boldsymbol{v}_i(t) = \frac{1}{2}(m_2 \boldsymbol{v}_2 \cdot \boldsymbol{v}_2 + m_3 \boldsymbol{v}_3 \cdot \boldsymbol{v}_3 + m_4 \boldsymbol{v}_4 \cdot \boldsymbol{v}_4) \tag{3.2}$$

and

$$\sum_{i=1}^{\text{links}} \frac{1}{2} I_i \dot{\theta}_i^2(t) = \frac{1}{2}(I_3 \dot{\theta}_3^2 + I_4 \dot{\theta}_4^2), \tag{3.3}$$

where all velocities are known from the computations of the previous section. In a general case, we would need to include the potential energy due to gravity

$$U(t) = \sum_{i=1}^{\text{masses}} m_i g h_i(t), \tag{3.4}$$

where g is gravity and h_i is a given datum height (from a reference). *However, this is not needed for a horizontal in-plane jab, although we will keep the term for completeness of the formulation*. From standard work–energy principles, we equate the sum of the kinetic and potential energy in an arbitrary 'configurational state 1' (at time $= t$), plus the work done from state 1 to a later (incremental) state, 'configurational state 2' (time $= t + \Delta t$, configuration 2) to yield

$$\begin{aligned}& T(t) + U(t) + \Delta W_{t \to t+\Delta t} - \Delta L_{t \to t+\Delta t} \\ & \quad = T(t + \Delta t) + U(t + \Delta t),\end{aligned} \tag{3.5}$$

where $\Delta W_{t \to t+\Delta t}$ is the incremental work done in moving the boxer's arm and fist, and $\Delta L_{t \to t+\Delta t}$ are the losses due to contact with the bag. This is enacted with $\boldsymbol{r}_2$ reaches a critical length to make contact. We can then immediately represent the incremental work as

$$\begin{aligned}\Delta W_{t \to t+\Delta t} = {} & (T(t + \Delta t) + U(t + \Delta t)) - (T(t) + U(t)) \\ & + \Delta L_{t \to t+\Delta t}.\end{aligned} \tag{3.6}$$

A relatively easy parametrization of the losses is (when in contact and the jab is moving forward)

$$\Delta L_{t \to t+\Delta t} = C(r_2(t + \Delta t) - r_2(t)), \tag{3.7}$$

where C is a loss coefficient per unit length, and $\Delta L_{t \to t+\Delta t} = 0$ otherwise (when the fist not in contact with the bag or the jab is retracting). We can then integrate[1]

$$W^{\text{tot}} = \text{energy expended} = \int_{t=t_1}^{t=t_2} \mathrm{d}W \approx \sum_{t=t_1}^{t=t_2} \Delta W. \tag{3.8}$$

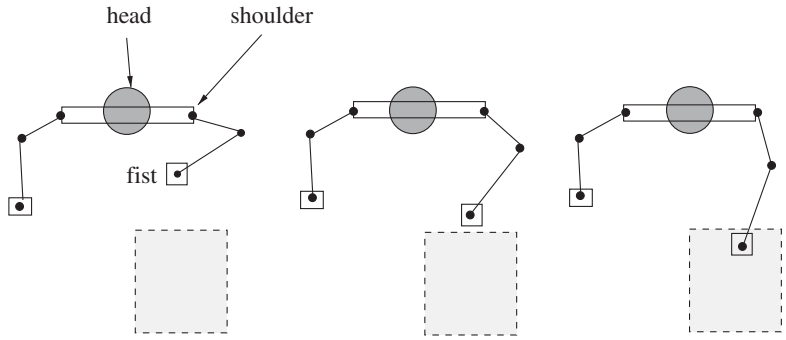

Figure 2. Top view of an in-plane jab.

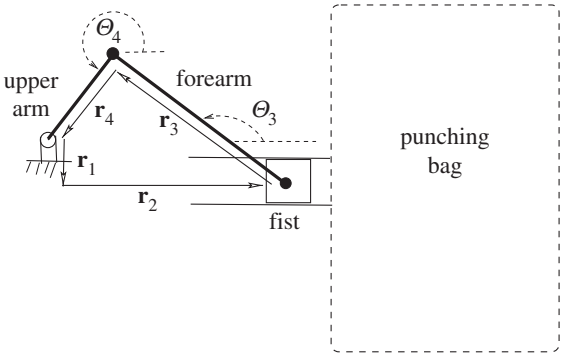

Figure 3. Linkage diagram for an (horizontal) in-plane left jab.

This gives the energy in joules. We can then convert into calories by $K_c = W^{tot}/4.184$ and into commonly used layman jargon 'calories', which are actually 'kilocalories' by kilo- $K_c = W^{tot}/4184$.

4. A numerical example: an hour-long workout

As an example, we consider the following parameters for an in-plane jab by using the average values of the range of a 75–100 kg male, from de Leva [17], Tozeren [18] and Plagenhoef *et al.* [19]:

— angular motion: $\theta_4, \dot{\theta}_4$ = controlled
— link 1 (offset) length: $r_1 = 0.05$ m,
— link 2 (location to fist) length: $r_2 = 0.25$ m (starting),
— link 3 (forearm) length: $r_3 = 0.3$ m,
— link 4 (upper arm) length: $r_4 = 0.25$ m,
— mass of link 2 (fist): $m_2 = 0.65$ kg,
— mass of link 3 (forearm): $m_3 = 1.5$ kg,
— mass of link 4 (upper arm): $m_4 = 2.5$ kg,
— location of the target (bag), $r_x = 0.4$ m.

The angular acceleration of link 4 during extension (from rest) is given by $\ddot{\theta}_4 = a_e = -100\,\mathrm{rad\,s^{-2}}$, and when retracting by $\ddot{\theta}_4 = a_r = 100\,\mathrm{rad\,s^{-2}}$. The total simulation time for a quick jab was approximately $T = 0.3$ s. The author is an amateur boxer, and these times and rates were determined from his own measurements. The linkage sequence is shown in figure 4. The loss coefficient (measured in joules/metre) is the one parameter that was varied, as it would depend on the type of obstacle being hit. We varied from 'shadow punches' (no resistance) to extremely heavy resistance: $C = 0, 1, 10, 10^2, 10^3, 10^4, 10^5, 10^6$. As the results in table 1, values of $C \leq 10^3$ burn extremely low numbers of calories. Between $10^3 \leq C \leq 10^5$ is a realistic range of parameters, while $C > 10^5$ results in expenditures that are unrealistic. The total kilocalories used in a single jab was computed, then to illustrate a 'mock' workout, we estimated a workout associated one jab every 5 s, thus 12 per min, thus 720 in 1 h. The incremental work done by the system is shown in figure 5 for the range $10^3 \leq C \leq 10^6$. One can see that upon contact with the body, the work rate jumps dramatically. It is important to emphasize that this is for a simple straight jab, and does not take into account other body motion. In order to more accurately compute biological energy expenditure one can use the concept of internal and external energy using muscle models, for example, found in [20,21]. The use of this type of framework to analyse more complex sports kinematics and the associated calorie expenditures is currently under investigation by the author. However, this will also require extensions to multi-limb movement, which we next discuss in the summary and extension section.

Remark. A variety of popular articles indicate that approximately 500–1000 calories are burned in a 1-h workout with a heavy bag for a 75–100 kg male [1–6]. This somewhat qualitative data would be interpreted for entire body movement, which we discuss next.

5. Summary and extensions for complex systems

The framework developed provides an analysis of a simple jab. Of course, in boxing and other contact sports, the motions can be much more complex, and will not lend themselves to closed form solutions. In particular, if one were to compute the dynamics of an entire body (figure 6), coupled vector loop systems will occur, and one must resort to numerical approaches. For example, in order to illustrate how numerical procedures are applied to such systems, consider again equation (1.1), which can be expressed in terms of its x- and y-components to form a nonlinear set of equations, which can be written as:

$$\begin{aligned} F_1(r_2,\theta_3) &\stackrel{\text{def}}{=} r_2\cos\theta_2 + r_3\cos\theta_3 \\ &= -r_1\cos\theta_1 - r_4\cos\theta_4 \stackrel{\text{def}}{=} R_1 \end{aligned} \tag{5.1}$$

and y-components

$$\begin{aligned} F_2(r_2,\theta_3) &\stackrel{\text{def}}{=} r_2\sin\theta_2 + r_3\sin\theta_3 \\ &= -r_1\sin\theta_1 - r_4\sin\theta_4 \stackrel{\text{def}}{=} R_2. \end{aligned} \tag{5.2}$$

These can be linearized for a Newton-iteration (i), for the x-components

$$\begin{aligned} F_1(r_2^{i+1},\theta_3^{i+1}) \approx F_1(r_2^i,\theta_3^i) &+ \left.\frac{\partial F_1}{\partial r_2}\right|_{r_2^i,\theta_3^i}(r_2^{i+1}-r_2^i) \\ &+ \left.\frac{\partial F_1}{\partial \theta_3}\right|_{r_2^i,\theta_3^i}(\theta_3^{i+1}-\theta_3^i) \end{aligned} \tag{5.3}$$

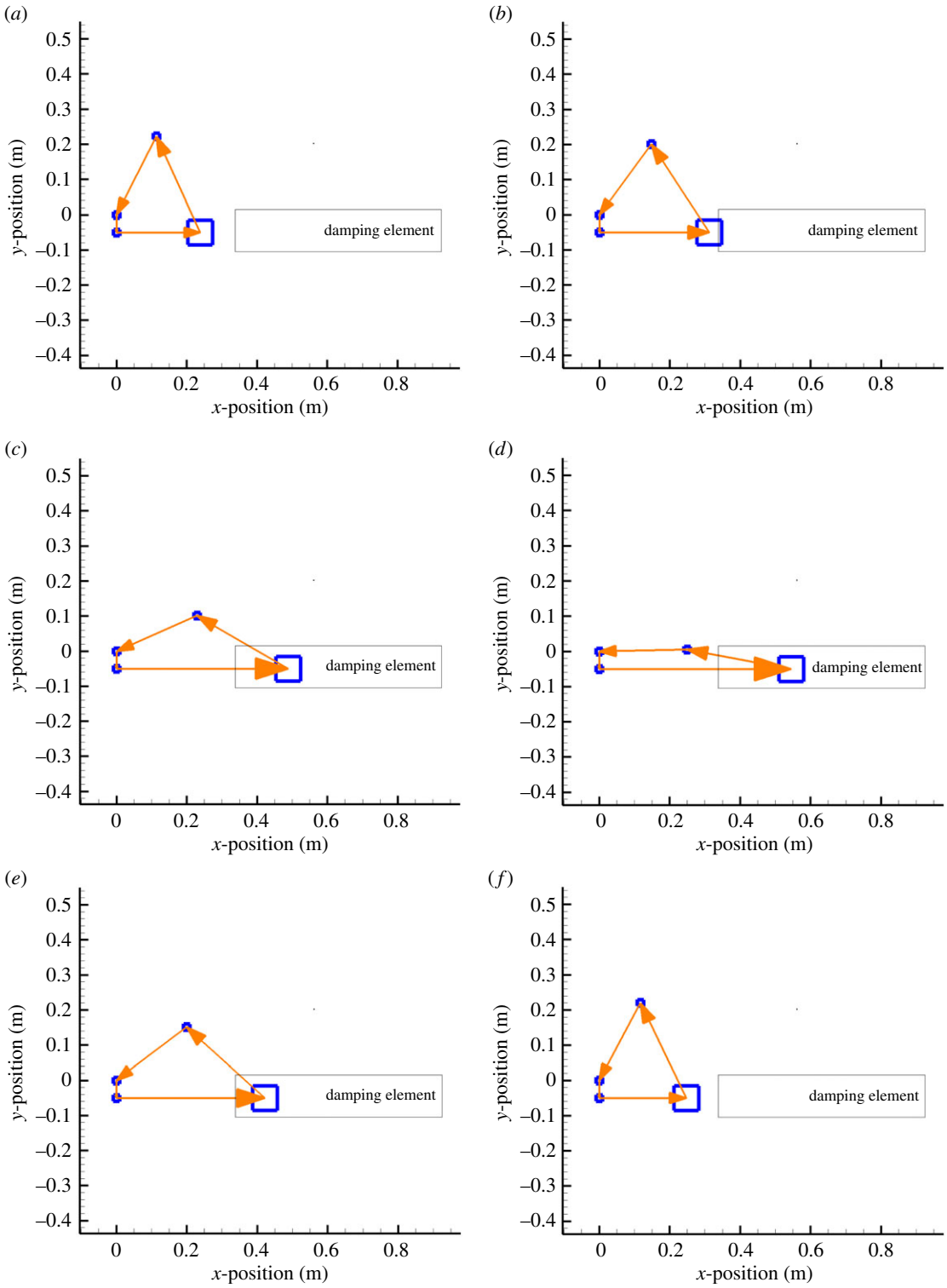

Figure 4. (*a–f*) Sequence of a punch to a bag at equal one-sixth interval times: $t = 0, T/6, T/3, T/2, T/6, T$, where T is the total time. The fist crossing into the box indicates that contact with the bag is taking place, accruing dissipation. The box is not the bag, it merely indicates when dissipation is taking place. (Online version in colour.)

and for the y-components

$$F_2(r_2^{i+1},\theta_3^{i+1}) \approx F_2(r_2^i,\theta_3^i) + \left.\frac{\partial F_2}{\partial r_2}\right|_{r_2^i,\theta_3^i}(r_2^{i+1}-r_2^i) + \left.\frac{\partial F_2}{\partial \theta_3}\right|_{r_2^i,\theta_3^i}(\theta_3^{i+1}-\theta_3^i). \tag{5.4}$$

In matrix form

$$\begin{bmatrix} \left.\frac{\partial F_1}{\partial r_2}\right|_{r_2^i,\theta_3^i} & \left.\frac{\partial F_1}{\partial \theta_3}\right|_{r_2^i,\theta_3^i} \\ \left.\frac{\partial F_2}{\partial \theta_3}\right|_{r_2^i,\theta_3^i} & \left.\frac{\partial F_2}{\partial r_2}\right|_{r_2^i,\theta_3^i} \end{bmatrix} \begin{Bmatrix} (r_2^{i+1}-r_2^i) \\ (\theta_3^{i+1}-\theta_3^i) \end{Bmatrix} = \begin{Bmatrix} R_1-F_1 \\ R_2-F_2 \end{Bmatrix}_{r_2^i,\theta_3^i}, \tag{5.5}$$

with the solution being

$$\begin{Bmatrix} (r_2^{i+1}-r_2^i) \\ (\theta_3^{i+1}-\theta_3^i) \end{Bmatrix} = \begin{bmatrix} \left.\frac{\partial F_1}{\partial r_2}\right|_{r_2^i,\theta_3^i} & \left.\frac{\partial F_1}{\partial \theta_3}\right|_{r_2^i,\theta_3^i} \\ \left.\frac{\partial F_2}{\partial \theta_3}\right|_{r_2^i,\theta_3^i} & \left.\frac{\partial F_2}{\partial r_2}\right|_{r_2^i,\theta_3^i} \end{bmatrix}^{-1} \begin{Bmatrix} R_1-F_1 \\ R_2-F_2 \end{Bmatrix}_{r_2^i,\theta_3^i}. \tag{5.6}$$

This can be solved at every increment, and is widely used in the analysis of robotic and kinematic systems involving large systems of coupled vector loops, such as those found in [7–16]. This multi-limb approach, coupled to the concept of internal and external energy using muscle models [20,21], is under current investigation by the author.

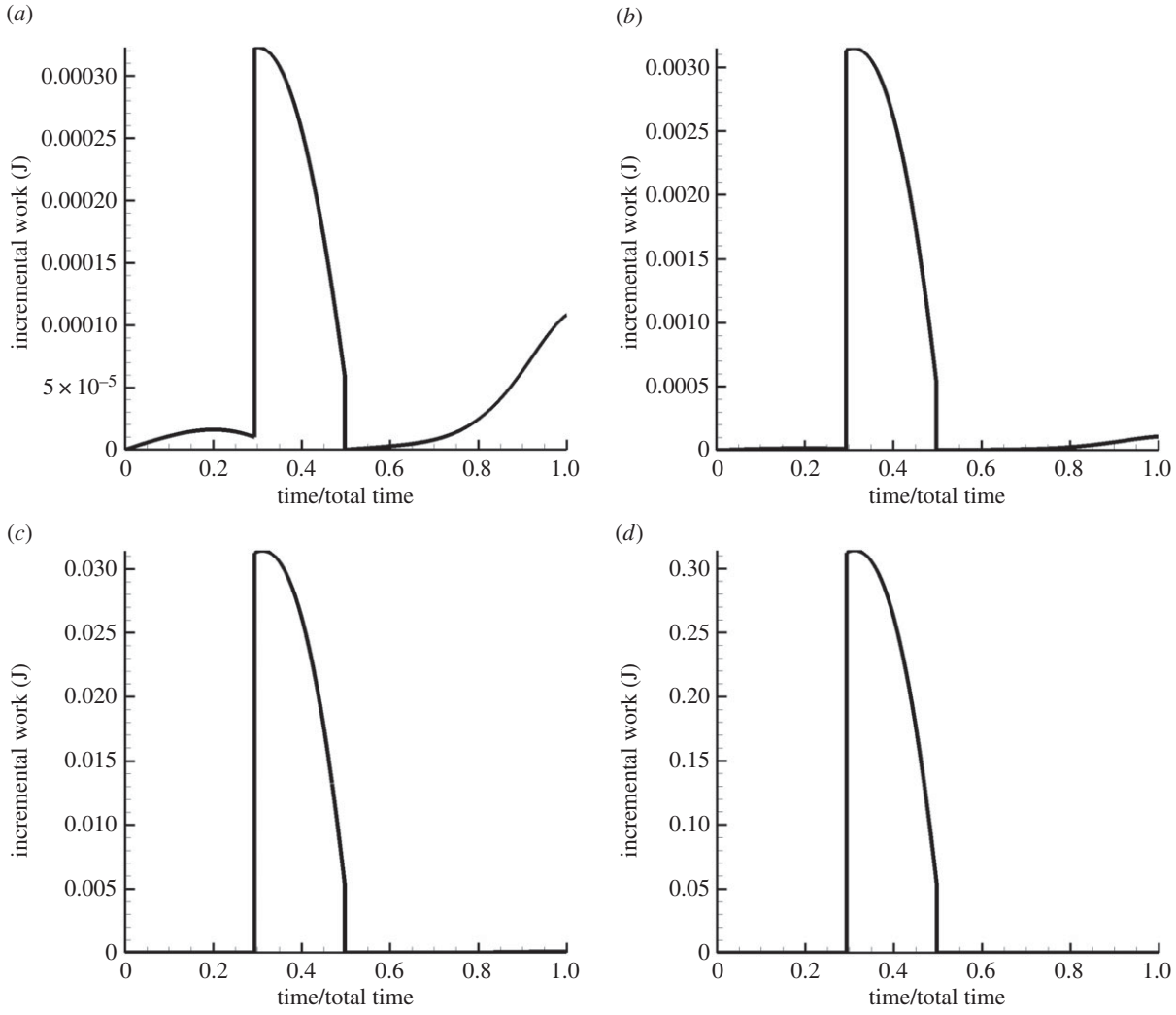

Figure 5. The incremental work (in joules), for various values of the loss-coefficient, (*a*) $C = 10$, (*b*) 10^2, (*c*) 10^3 and (*d*) 10^4. The spike occurs when contact is made with the object, with the decrease resulting upon retraction of the 'fist'.

Table 1. The calories expended for various values of the loss-coefficient, $C = 0, 1, 10, 10^2, 10^3, 10^4, 10^5, 10^6$.

loss coeff.: *C*	kilocalories/jab	total kilocalories (720 jabs)
0	0.0134	9.711
1	0.0135	9.723
10	0.0136	9.839
10^2	0.0165	11.934
10^3	0.0480	34.591
10^4	0.3627	261.155
10^5	3.5094	2526.797
10^6	34.9767	25183.215

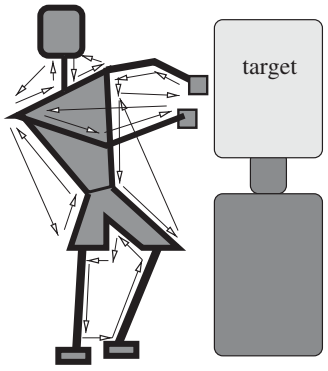

Figure 6. Hypothetical multiple coupled vector loops that must be solved numerically.

Finally, a further point of investigation is the correlation of body blows to accelerated atherosclerosis and general artery stenosis in ageing boxers (as well as in participants in other contact sports). The approach is to couple recent models found in [22–25], which describe the accumulation of microscale materials at solid–fluid interfaces in biological channels. This is often the initial stage of biochannel occlusive growth processes [26–30].[2] In those models, the approach is to construct rate equations for the accumulation of suspended materials in the bloodstream at the solid–fluid interface. The accumulation of material subsequently reduces the cross-sectional area of the channel, which can lead to dementia-like symptoms commonly associated with older boxers (such observations date back, at least, to Mawdsley & Ferguson [45] and with relatively recent data collected in Krishnan [46]). The generation and deposition of calcium and fatty deposits on channel walls is an open question of increasing interest [47–50], and the repeated

blows from contacts sports has been hypothesized to enhance such growth. A future objective is to use kinematic models, such as the one developed here, to simulate a wide range of induced forces involving fist-to-head and fist-to-chest force calculations and to determine the connections to possible accelerated biological channel growth.

Competing interests. We declare we have no competing interests.

Funding. We received no funding for this study.

Endnotes

[1]If the angular velocity of link 4 is controlled by a moment (the source of power), then $M_4(t)\Delta\theta_4(t) = \Delta W(t)$.
[2]For surveys of plaque-related work, see [31–44].

References

1. Thompson S. 2013 Calories burned while boxing with a heavy bag. See http://www.livestrong.com/article/541231-calories-burned-while-boxing-with-a-heavy-bag/.
2. Mccoy W. 2014 Calories burned boxing. See http://www.livestrong.com/article/293553-calories-burned-boxing/.
3. Wolfe L. 2015 Shadow boxing to lose weight. See http://www.livestrong.com/article/358216-shadow-boxing-to-lose-weight/.
4. Wayne J. 2014 How to practice boxing at home. See http://www.livestrong.com/article/413615-how-to-practice-boxing-at-home/
5. Miller SJ. 2013 Compare calories of cardio boxing to running. Livestrong.com: See http://www.livestrong.com/article/552192-compare-calories-of-cardio-boxing-to-running/
6. Narins E. 2014 11 workouts that burn more calories than jogging. See http://www.cosmopolitan.com/health-fitness/advice/a29580/workouts-that-burn-more-calories-than-jogging/
7. Hunt KH. 1979 *Kinematic geometry of mechanisms*. Oxford Engineering Science Series. Oxford, UK: Oxford University Press.
8. Hartenberg RS, Denavit J. 1964 *Kinematic synthesis of linkages*. New York, NY: McGraw-Hill.
9. Howell LL. 2001 *Compliant mechanisms*. New York, NY: John Wiley & Sons.
10. McCarthy JM, Soh GS. 2010 *Geometric design of linkages*. New York, NY: Springer.
11. McCarthy JM. 1990 *Introduction to theoretical kinematics*. Cambridge, MA: MIT Press.
12. Reuleaux F. 1876 *The kinematics of machinery*. (trans. and annotated by A. B. W. Kennedy), reprinted by Dover, New York (1963).
13. Sandor GN, Erdman AG. 1984 *Advanced mechanism design: analysis and synthesis*, vol. 2. Englewood Cliffs, NJ: Prentice-Hall.
14. Slocum A. 1992 *Precision machine design*. SME.
15. Suh CH, Radcliffe CW. 1978 *Kinematics and mechanism design*. New York, NY: John Wiley and Sons.
16. Uicker JJ, Pennock GR, Shigley JE. 2003 *Theory of machines and mechanisms*. New York, NY: Oxford University Press.
17. deLeva P. 1996 Adjustments to Zatsiorsky-Seluyanov's segment inertia parameters. *J. Biomech.* **29**, 1223–1230. (doi:10.1016/0021-9290(95)00178-6)
18. Tozeren A. 2000 *Human body dynamics*. Berlin, Germany: Springer.
19. Plagenhoef S, Evans FG, Abdelnour T. 1983 Anatomical data for analyzing human motion. *Res. Q. Exerc. Sport* **54**, 169–178. (doi:10.1080/02701367.1983.10605290)
20. Winter DA. 2016 A new definition of mechanical work done in human movement. *J. Appl. Physiol. Respir. Environ. Exerc. Physiol. 1979* **46**, 79–83.
21. Böhm B, Hartmann M, Böhm H. 2016 Body segment kinematics and energy expenditure in active videogames. *Games Health* **5**, 189–196. (doi:10.1089/g4h.2015.0058)
22. Zohdi TI. 2014 Mechanically-driven accumulation of microscale material at coupled solid–fluid interfaces in biological channels. *J. R. Soc. Interface* **11**, 20130922. (doi:10.1098/rsif.2013.0922)
23. Zohdi TI. 2005 A simple model for shear stress mediated lumen reduction in blood vessels. *Biomech. Model. Mechanobiol.* **4**, 57–61. (doi:10.1007/s10237-004-0059-2)
24. Zohdi TI. 2004 A computational framework for agglomeration in thermo-chemically reacting granular flows. *Proc. R. Soc. Lond. A* **460**, 3421–3445. (doi:10.1098/rspa.2004.1277)
25. Zohdi TI, Holzapfel GA, Berger SA. 2004 A phenomenological model for atherosclerotic plaque growth and rupture. *J. Theor. Biol.* **227**, 437–443. (doi:10.1016/j.jtbi.2003.11.025)
26. Ambrosi D *et al.* 2011 Perspectives on biological growth and remodeling. *J. Mech. Phys. Solids* **59**, 863–883. (doi:10.1016/j.jmps.2010.12.011)
27. Göktepe S, Abilez OJ, Parker KK, Kuhl E. 2010 A multiscale model for eccentric and concentric cardiac growth through sarcomerogenesis. *J. Theor. Biol.* **265**, 433–442. (doi:10.1016/j.jtbi.2010.04.023)
28. Menzel A, Kuhl E. 2012 Frontiers in growth and remodeling. *Mech. Res. Comm.* **42**, 1–14. (doi:10.1016/j.mechrescom.2012.02.007)
29. Kuhl E, Maas R, Himpel G, Menzel A. 2007 Computational modeling of arterial wall growth: attempts towards patient specific simulations based on computer tomography. *Biomech. Model. Mechanobiol.* **6**, 321–331. (doi:10.1007/s10237-006-0062-x)
30. Zöllner AM, BuganzaTepole A, Kuhl E. 2012 On the biomechanics and mechanobiology of growing skin. *J. Theor. Bio.* **297**, 166–175. (doi:10.1016/j.jtbi.2011.12.022)
31. Chyu KY, Shah PK. 2001 The role of inflammation in plaque disruption and thrombosis. *Rev. Cardiovas. Med.* **2**, 82–91.
32. Davies MJ, Richardson PD, Woolf N, Katz DR, Mann J. 1993 Risk of thrombosis in human atherosclerotic plaques: role of extracellular lipid, macrophage, and smooth muscle cell content. *Br. Heart J.* **69**, 377–381. (doi:10.1136/hrt.69.5.377)
33. Fuster V. 2002 *Assessing and modifying the vulnerable atherosclerotic plaque*. Armonk, NY: Futura Publishing Company.
34. Kaazempur-Mofrad MR, Wada S, Myers JG, Ethier CR. 2005 Blood flow and mass transfer in arteries with axisymmetric and asymmetric stenoses. *Int. J. Heat Mass Transf.* **48**, 4510–4517. (doi:10.1016/j.ijheatmasstransfer.2005.05.004)
35. Kaazempur-Mofrad MR, Younis HF, Isasi AG, Chan RC, Hinton DP, Sukhova G, LaMuraglia GM, Lee RT, Kamm RD. 2004 Characterization of the atherosclerotic carotid bifurcation using MRI, finite element modeling and histology. *Ann. Biomed. Eng.* **32**, 932–946. (doi:10.1023/B:ABME.0000032456.16097.e0)
36. Kaazempur-Mofrad MR, Younis HF, Patel S, Isasi AG, Chung C, Chan RC, Hinton DP, Lee RT, Kamm RD. 2003 Cyclic strain in human carotid bifurcation and its potential correlation to atherogenesis: idealized and anatomically-realistic models. *J. Eng. Math.* **47**, 299–314. (doi:10.1023/B:ENGI.0000007974.82115.16)
37. Libby P. 2001 Current concepts of the pathogenesis of the acute coronary syndromes. *Circulation* **104**, 365–372. (doi:10.1161/01.CIR.104.3.365)
38. Libby P. 2001 The vascular biology of atherosclerosis. In *Heart disease. A textbook of cardiovascular medicine*, sixth, ch. 30 (eds E Braunwald, DP Zipes, P Libby), pp. 995–1009. Philadelphia, PA: W. B. Saunders Company.
39. Libby P, Ridker PM, Maseri A. 2002 Inflammation and atherosclerosis. *Circulation* **105**, 1135–1143. (doi:10.1161/hc0902.104353)
40. Libby P, Aikawa M. 2002 Stabilization of atherosclerotic plaques: new mechanisms and clinical targets. *Nat. Med.* **8**, 1257–1262. (doi:10.1038/nm1102-1257)
41. Loree HM, Kamm RD, Stringfellow RG, Lee RT. 1992 Effects of fibrous cap thickness on peak circumferential stress in model atherosclerotic vessels. *Circ. Res.* **71**, 850–858. (doi:10.1161/01.RES.71.4.850)

42. Richardson PD, Davies MJ, Born GVR. 1989 Influence of plaque configuration and stress distribution on fissuring of coronary atherosclerotic plaques. *Lancet* **2**, 941–944. (doi:10.1016/S0140-6736(89)90953-7)
43. Shah PK. 1997 Plaque disruption and coronary thrombosis: new insight into pathogenesis and prevention. *Clin. Cardiol.* **20**(Suppl. II), II-38–II-44.
44. van der Wal AC, Becker AE. 1999 Atherosclerotic plaque rupture—pathologic basis of plaque stability and instability. *Cardiovasc. Res.* **41**, 334–344. (doi:10.1016/S0008-6363(98)00276-4)
45. Mawdsley C, Ferguson FR. 1963 Neurological disease in boxers. *Lancet* **282**, 795–801. (doi:10.1016/S0140-6736(63)90498-7)
46. Krishnan V. 2011 *Forensic medicine and toxicology*. Amsterdam, The Netherlands: Elsevier.
47. Weinberg EJ, Schoen FJ, Mofrad MRK. 2009 A computational model of aging and calcification in the aortic heart valve. *PLoS ONE* **4**, e5960. (doi:10.1371/journal.pone.0005960)
48. Wenk JF, Papadopoulos P, Zohdi TI. 2010 Numerical modeling of stress in stenotic arteries with microcalcifications: a micromechanical approximation. *J. Biomech. Eng.* **132**, 091011-1–11. (doi:10.1115/1.4001351)
49. Klepach D, Lee LC, Wenk J, Ratcliffe M, Zohdi TI, Navia J, Kassab G, Kuhl E, Guccione JM. 2012 Growth and remodeling of the left ventricle: a case study of myocardial infarction and surgical ventricular restoration. *Mech. Res. Commun.* **42**, 134–141. (doi:10.1016/j.mechrescom.2012.03.005)
50. Lee LC *et al.* 2013 Analysis of patient-specific surgical ventricular restoration—importance of an ellipsoid left ventricular geometry for diastolic and systolic function. *J. Appl. Physiol.* **115**, 136–144. (doi:10.1152/japplphysiol.00662.2012)